PHOTOCATALYTIC DEGRADATION OF CHLORAMPHENICOL USING HYDROXYAPATITEDERIVED FROM EGG SHELLS

Amiel Clark G. Cabotaje, Ariana Camille C. Teodoro, Lorraine S. Climaco, Engr. Rugi Vicente D. Rubi & Engr. Jerry G. Olay[1]

Department of Chemical Engineering, College of Engineering, Adamson University, Ermita, Manila, Philippines

[1]jerry.olay@adamson.edu.ph

Abstract

This paper investigated the photocatalytic degradation of Chloramphenicol using hydroxyapatite derived from eggshells via microwave--assisted synthesis. The photocatalytic degradation of Chloramphenicol was conducted under different parameters such as varying irradiation time for catalyst (10, 20 and 30 minutes), catalyst loading (0.4, 0.6 and 0.8 mg), and time exposure (0.5, 1.0, 1.5, 2.0 and 2.5 hours). Chicken and duck eggshells are composed of calcium carbonate that is synthesized into hydroxyapatite by mixing with diammonium phosphate, $(NH_4)_2HPO_4$, under microwave irradiation. Characterizations confirmed that the properties of the synthesized product are in line with the properties that is generally known as HA, in accordance to the data of characterizing the said catalyst presented from other studies. Also, the comparison of the different parameters of photocatalytic degradation showed the use of initial pollutant concentration of 25 mg/L with a catalyst loading of 0.8 mg HA with irradiation time 20 minutes in microwave under UV lights for 2.5 hours gave the most promising result, giving a percent degradation of Chloramphenicol approximately 80.92%. Overall, this study provided insight on the possible use of a waste material, particularly eggshells, as a source of HA and possibly, a greener way of handling wastewater.

Keywords: Calcination, Chloramphenicol, Photocatalytic Degradation, Hydroxyapatite, Eggs

1.0 INTRODUCTION

Conventional wastewater treatment plants have limitations in treating antibiotics in wastewater because of its antibiotic effects and high molecular complexity. In addition, the elimination of drug residues and metabolites has been one of the difficulties encountered in the usage of conventional wastewater treatment plants since these factors cannot be completely removed from wastewater that contain antibiotics. Hence, there is a serious necessity in improving wastewater treatments. (Autónoma et al., 2011) Among all the technologies used for the removal of antibiotics in wastewater, photocatalytic degradation has been of great interest. In photocatalytic degradation, a photocatalyst is used to separate the contaminant with water. The photocatalyst together with the contaminant is illuminated by light. There were studies on the treatment of chloramphenicol in wastewater using photocatalytic degradation and TiO_2 as the photocatalyst. TiO_2 is a well--known photocatalyst because of its effectiveness on the removal of contaminant. It is also cheap and readily available. However, there are also limitations in using TiO_2 as photocatalyst. Its limitations include the ineffective mistreatment of visible light;; its low adsorption capability for hydrophobic contaminants;; its uniform diffusion in aqueous suspension;; and post recovery of the TiO_2 elements after water treatment (Dong et al., 2015).

This study focused on CAP degradation using Hydroxyapatite, $Ca_{10}(PO_4)_6(OH)_2$, as a photocatalyst. Hydroxyapatite in general is a main constituent for all human's bones. That is why it is mostly used on orthopedic, dental, and maxillofacial applications. In addition, hydroxyapatite does not contain any toxicity since it was produced from biogenic sources. In photocatalytic activity of hydroxyapatite, it was found out that hydroxyapatite has great sorption activities that is useful for the degradation of antibiotics. HA synthesis can be achieved by different methods such as chemical precipitation, sol--gel method, solid--state reaction, etc. (Shavandi et al., 2014).

2.0 LITERATURE REVIEW

The hydroxyapatite is naturally produced from calcium with the formula $Ca_5(PO_4)_3(OH)$. It is commonly was wrote as $Ca_{10}(PO_4)_6(OH)_2$. It is usually found in teeth, bones, and tendons of the human body that give these organs hardness and stability. Its biocompatibility is due to its chemical analogy with the biological tissue. (Kumar et al., 2012).

There are different methods in the preparation of HA in literature. Over the past decade, different synthetic techniques were developed for the preparation of HA considering the technique's scientific and economic features. There were also studies on the properties of HA on how varying parameters can affect the properties. (Sadat--shojai, et al., 2013).

Among other methods, microwave irradiation can synthesize HA faster than any other methods. It also offers simple reproducibility, narrow particle distribution, high purity, high yield, throughout volume heating and efficient energy transformation. It can also offer fast and shorter time of synthesis that causes thermal gradients to minimize and

lessen the time for particle diffusion;; therefore in shorter time, the HA can be produced (Sajahan et al., 2014).

Hydroxyapatite can be derived from different bio--waste products like mussel shells, clamshells, and eggshells (as in the present study). Physical properties like phase purity, particle size, and shape of HA are considered (Shavandi, et al. 2016). Shavandi et al., (2016) investigated the conversion of waste shells in HAp.

In most studies on characterization of hydroxyapatite, XRD is used to mark crystalline peaks. It uses double nature wave or particle of the X--rays in order to determine the structure of the materials. It usually works when the beam of monochromatic X--rays reacted within the sample scatters the X--rays from the atoms through the sample. In a study of Teoreanu et al., (2008), hydroxyapatite was characterized by XRD. Hydroxyapatite's crystalline phase was determined by X--ray patterns diffraction using CuKa radiation (Shimadzu XRD Diffractometer) before the thermal process and after.

SEM is an electronic image of kind of samples is produced through scanning with a focused beam of electrons. In a study of Malakauskaite--Petruleviciene et al., (2015), SEM was used to observe morphological features on calcium hydroxyapatite. Hitachi SU--70 scanning electron microscope was used. Layers of 1, 5, 15, and 30 was observed in the SEM micrographs of calcium hydroxyapatite. Changes in the surface morphology of calcium hydroxyapatite were observed under increasing spinning time. Reddy et al., (2007), characterized HA using JEOL--JSM 5600 instrument.

FT--IR used to obtain an infrared spectrum of absorption or emission of any material. The mechanism of FTIR starts by the collection of high rise of spectral solution data which over a wide range spectral of the spectrometer. Singh, (2012) characterized hydroxyapatite to study its spectral characteristics including its chemical bonding. Results showed the presence of –OH bond. It also confirmed the presence of PO_4^{3--} group in HA.

Chloramphenicol, $C_{11}H_{12}Cl_2N_2O_5$, is an antibiotic used to treat different illnesses like meningitis, plague, cholera, typhoid fever. Due to its side effects, chloramphenicol is only advisable if there are no other safer antibiotics available. The side effects of chloramphenicol are bone marrow suppression, nausea, and diarrhea. It is an antibiotic from cultures of Streptomyces venequelae. It intervenes with protein authorship of positive and negative gram--bacteria (Dfs, et al., n.d.).

Among all wastewater treatments, photocatalytic degradation has been an emerging technique in removing contaminants. Its advantages include: no problems for waste disposal, cheaper than other kind of treatment and complete mineralization (Bhatkhande, Pangarkar, and Beenackers, 2002).

3.0 METHODOLOGY

Materials and Methods

The eggshells were obtained from an egg factory in Bulacan. The researcher bought rejected eggs from the factory and utilized the eggshells in the experiment.

EDTA 99.4% (Ethylenediaminetetraacetic Acid), ($C_{10}H_{16}N_2O_8$) 0.1 M was used as a material bought from LOBA CHEMIE PVT. LTD in India. Sodium phosphate dibasic 99%--101% (Na_2HPO_4) 0.6 reagent was purchased from UNIVAR in Singapore;; and Whatman Filter papers from Germany with 42 micrometer Porosity.

The collected eggshells were cleaned by boiling it into the water for 15--20 minutes to remove all the inner membrane and other possible contaminants.

The wet method used MAE standard method to prepare the HA by using EDTA complex as explained by (Liu et al., 2004) and (Sajahan et al., 2014). The cleaned eggshells were subjected to two stages of thermal process. The first stage was heating the eggshells at 450°C for 2hrs. The rate of heating was controlled by increasing 5°C/min until reaching 450°C. During that stage, organic remainders were expected to be eradicated. The second stage was heating up to 900°C for 2hrs. The rate of heating was controlled by increasing 5°C/min. The eggshells were converted into calcium oxide (CaO) by the discharge of carbon dioxide in that temperature. The calcium oxide obtained were grounded by mortar and pestle. Three (3) grams of calcium oxide were mixed with 50mL of 0.1M EDTA (0.1M EDTA were prepared by dissolving 29.224g of $C_{10}H_{16}N_2O_8$ in 1L of DI water), to form an EDTA complex. The solution was added with 50mL of 0.6M Na_2HPO_4 (0.6M Na_2HPO_4 were prepared by dissolving 14.196g of the raw powder in 1L of DI water) and stirred for fifteen (15) minutes. The initial pH was maintained at a value of thirteen (13). The addition of NaOH or H_2SO_4 was used to adjust the pH. However, it was expected that the pollutant was able to maintain its pH level at approximately thirteen (13) without any adjusting. The solution was placed in the Laboratory Grade Microwave (Microwave-- BP090), and irradiated with 30% microwave power used for the heating of HA to produce HA powder for 10, 20, and 30mins. The precipitate formed was washed thoroughly with deionized water to eliminate possible remaining Na^+ and EDTA. Afterwards, it was dried in the oven for seven (7) hours at 80°C to acquire the HA powder.

The spiked chloramphenicol wastewater solution was prepared by dissolved 1000 milligrams of chloramphenicol ($C_{11}H_{12}Cl_2N_2O_5$) powder in 1L of DI water to formulate 3mM CAP (1000mg/L) solution. Thereafter, it was subjected to a series of dilution to achieve the desired concentration of 25 mg/L based on the maximum appeared of chloramphenicol in wastewater from EPA (Environmental Protection Agency) (Dfs et al.,) and (Bhatkhande, Pangarkar, and Beenackers,) which can be done using a normal dilution equation. (See 2.1;;2.2;;2.3)

$$V_1 C_1 = V_2 C_2 \quad (2.1)$$

$$V_1 * 1000 = 25 * 200 \quad (2.2)$$

$$V_1 = 5mL \quad (2.3)$$

Adding 5ml of 1000ppm of CAP to 195ml of DI water gave a 200ml of 25ppm of CAP. After preparing enough pollutant for the experiment, 1000ppm was used to prepper other pollutant with different concentrations as 5mg/L, 10mg/L, 15mg/L, 20mg/L and 30mg/L. The UV--Vis was used to test the quality and concentration of chloramphenicol solution in different concentrations to construct the calibration curve.

Photocatalytic Degradation of Chloramphenicol

Photocatalytic degradation of CAP was conducted at room temperature in 300mL Pyrex vessel. HA powder with different amount of 0.4, 0.6, and 0.8 g were mixed into the prepared spiked chloramphenicol solution at natural pH of 5.5 to produce several independent test samples. Each mixture was stirred using the magnetic stirrer immersed in the samples before and during the UV light exposure. The mixtures were kept in the dark for about 30 mins to attain maximum adsorption of CAP in the HA surface before the UV irradiation. UV lamp was used for the irradiation at a normal power of 6W. The sample was exposed to UV light at various time intervals of 30 mins, 1hr., 1.5hr., 2hr., and 2.5 hrs. For kinetic studies, 5mL of sample was withdrawn at various time intervals. Moreover, the kinetic study was assumed the photocatalytic degradation to follow the pseudo--first--order (Ahmadi et al., 2017) and (Elmolla and Chaudhuri, 2010).

Removal of Chloramphenicol from Spiked Chloramphenicol Wastewater Solution

After the degradation of CAP using HA powder as catalyst, the solution was filtered using Whatman filter paper to separate the HA particles from the reacted solution. The filtrate was then tested by UV--Vis to examine the change in concentration of CAP in the sample and FT--IR to analyze the solid filtrate after the degradation process to distinguish all the peaks extend in all HA groups.

Statistical Analysis

The ANOVA was used to detect the effect of the variation of parameters in the said treatments. The spiked chloramphenicol solution was tested using UV--Vis. The results will be used to determine the effects of the variation of time and concentration of the catalyst to the degradation of the said antibiotic Two--way ANOVA was used to determine the significance of the catalyst loading during all different times of exposure. All ANOVA calculations were done using Minitab 18.

4.0 RESULTS AND DISCUSSION

Characterization of Hydroxyapatite

Fourier Transform Infrared (FTIR) Spectrum

The three batches of hydroxyapatite were tested for each kind of irradiation, and were irradiated for 10, 20 and 30 minutes in the microwave. These were compared from the other study to determine the HA functional groups (OH and PO_4). This study illustrated the three catalysts with different irradiation times. The FTIR results show the bond peaks between the range 3670cm^{-1} to 545cm^{-1}.

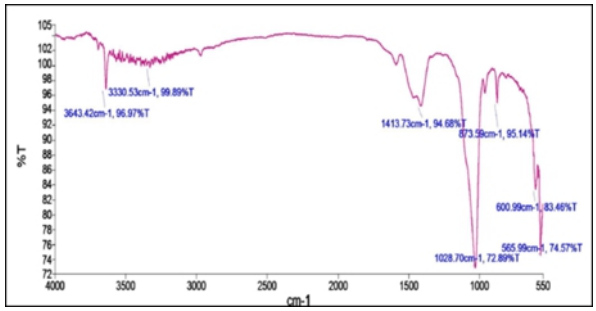

Figure 1: The FTIR result of the derived hydroxyapatite HA which was irradiated for 20 minutes in the microwave

The FTIR spectrum confirmed the functional groups of HA (Lin et al., 2017). All the peaks were listed as 3643.42 cm^{-1}, 3330.53 cm^{-1}, and 500.98 cm^{-1} all falling between 3670 cm^{-1} to 3573 cm^{-1}, 3570cm^{-1} to 3320 cm^{-1}, and 640 cm^{-1} to 600 cm^{-1} respectively, this confirms the presence of hydroxyl group (OH) that point out the existence of HA (Berzina--Cimdina and Borodajenko, 2012). Further it shows the strongest peaks for HA which was irradiated for 20 minutes at 3330.53 cm^{-1} between 3570 cm^{-1} to 3320cm^{-1} based on the standard peaks of the phosphate group (PO_4^{3-}). Phosphate groups can be also found at 1028.70 cm^{-1} and 565.99 cm^{-1}. Additionally, the peak at 1413 cm^{-1} verified the phosphate ion (Tkalčec, Popović, Orlić, Milardović, and Ivanković, 2014).

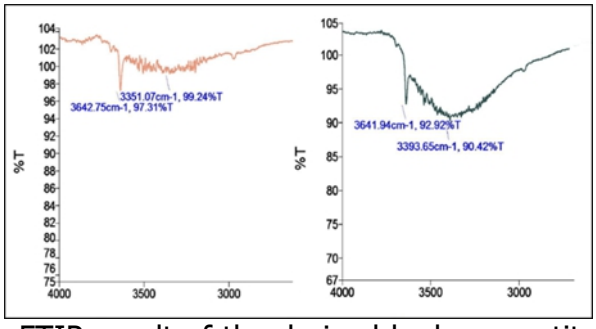

Figure 2: The FTIR result of the derived hydroxyapatite HA which was irradiated for 10 and 30 minutes in the microwave

Figure 2 shows the first peaks for OH group 3642 cm^{-1} and 3641 cm^{-1} falling between 3670 cm^{-1} to 3573 cm^{-1},, and the other peaks at 3351 cm^{-1} and 3393 cm^{-1} falling between 3570 cm^{-1} and 3393 cm^{-1}. Herewith, the sample with an irradiation time of 20 minutes was in between the range of those peaks that manifest the functional groups for HA.

Scanning Electron Microscopy (SEM)

The HA was observed at close range as shown on Figure 3 for each irradiation time. SEM images were taken at lower and higher magnification using Scanning Electron Microscopy (JSM--5310, Tokyo Japan) to analyze particle size and surface topography after coater using JEOL JFC--1200. As described by its operation (Iqbal et al., 2017), the instrument was operated at 20 kV acceleration voltage. The sample was tinted in a cathodic evaporator which had a gold layer 20 nm thick.

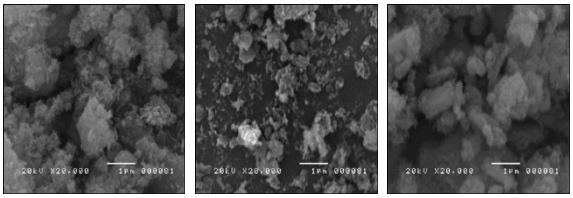

Figure 3: SEM analysis at lower magnification (10, 20, and 30 mins irradiation)

In Figure 3, shows that HA is mainly established of stacking heaps of agglomerates and particle with irregular--shaped (Rivera et al., 1999). This was due to the increase in irradiation time caused by the decreased in the particle size of the catalyst as shown on Figure 3. The samples with the irradiation time of 20 and 30 minutes showed micrometrical particles that were immensely agglomerated endorse its morphology in terms of blocks. Furthermore, the comparison between all irradiation levels showed that the particle size increases along with the irradiation time (Iqbal et al., 2017).

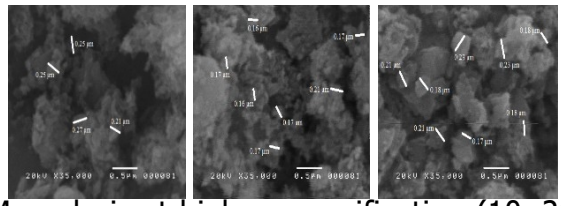

Figure 4: SEM analysis at higher magnification (10, 20, and 30 mins irradiation)

The powderized HA exhibited the collective amount in formation of agglomeration heaps of the crystals of the powderized sample. It was in irregular shape formation because of its structure during the heat applied at 900°C. Furthermore, it presents the synthesized of HA powder was described as nanoparticles (having the size that can be characterized within the range of 10--1000 nanometers) and microparticles (having the size that can falls within the range of 0.1--1 micrometers) for HA with 10 minutes irradiation the particles size were falling in at the same range with average of 0.24 micrometer;; and 0.17 micrometer as an average for the HA particles with 20 minutes irradiation;; and the HA particles which irradiated for 30 minutes gave an average size 0.19 micrometer. Moreover, all samples had non--uniform particles with a size that can have relatively. average size as 210 nanometer (Iqbal et al., 2017).

X- -Ray Diffraction (XRD)

The HA powder was tested using Shimadzu Maxima XRD--7000. The sample was powdered using a quartz agate before being installed on the XRD sample's holder and maximizing the consistency of signals around the HA crystalline faces. Then, it went through a full scan X--Ray diffraction analysis series from 3.0° to 90°p, 2θ/θ angle. The Cu--Kα was the source of radiation for generating X--ray beams (40 kV;; 30 mA) at a wavelength of 1.54Å to compute for the inter--atomic spacing (d--values) using Bragg's equation. The decision parameter for this analysis was specified at 0.02 °, with scan speed maintained at 20° per minute. The detection limit is 5% and strongly dependent on the crystallinity.

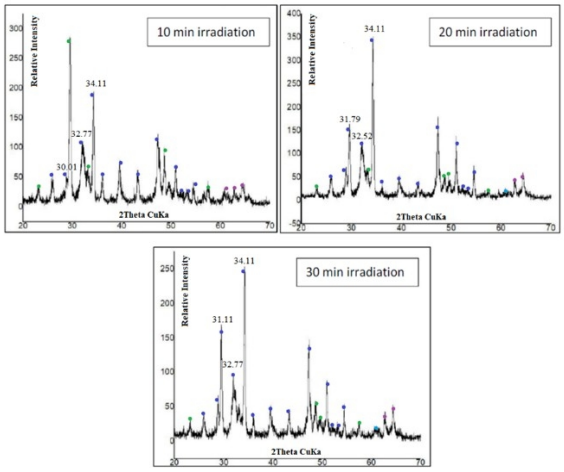

Figure 5: The XRD patterns of synthesized hydroxyapatite which were irradiated for (a) 10 minutes, (b) 20 minutes, and (c) 30 minutes

The 20 and 30 minutes irradiated samples showed all three highest peaks (2θ) as observed from the synthesized HA such as 32.77°, 31.79°, and 34.11°, respectively. Futhermore, the three results appeared to be in accordance with the results of the works of Abo--Almaged and Gaber which reported that hydroxyapatite formation can be found in the major peaks at;; 2θ ~ 32.7°, 2θ ~ 31.8° and 2θ ~34.1°.

Application of Photocatalysis for Deradation

The adsorption rate for the photocatalytic degradation of CAP was shown by the UV--Vis. The concentration rates were calculated from the adsorption rate of CAP. The concentration of CAP all throughout the experiment was 25 $mg.L^{-1}$. All the results from the UV--Vis were achieved at the maximum wavelength of 275nm, the highest peaks were found in range 272nm to 275nm while the adsorption rate was calculated. The hydroxyapatite with 20 minutes irradiation time in the microwave was used to degrade CAP during the experiment.

Table 1: The concerntration of CAP in all degradation levels

Photocatalytic Degradation of Chloramphenicol (CAP)								
		UV Light exposure of HA (Concentration)						
Conc. of CAP (mg/L)	**Conc. of HA solution (g)**	Irradiation Time for HA Powder (minutes)	0 minutes	30 minutes	1 Hour	1.5 Hours	2 hours	2.5 hours
25	0.4	20	24.95	16.21	12.65	10.82	9.14	8.85
25	0.6	20	24.95	15.07	9.99	9.71	7.66	7.35
25	0.8	20	24.95	12.65	10.54	7.66	6.09	4.76

The different amount of catalyst loadings such as 0.4g, 0.6g, and 0.8g were dosed with 250ml of pollutant with 25 $mg.L^{-1}$ concentration. Lastly, time exposure under UV lights was also assorted with different times 0, 30, 60, 90, 120 and 150 minutes.

Table 1, presents that the highest degradation of CAP noted after 150 minutes of exposure with 80.92% degradation efficiency were obtained using 0.8 g of HA which was synthesized under 20 minutes irradiation.

The trend attained by the catalyst dosages from 0.4 to 0.8 grams were increasing in direct proportion. Furthermore, the increase in efficiency implies that the catalyst is more capable of adsorbing the pollutant by increasing its initial concentration (Hassena, 2016). However, increasing the initial amount of catalyst loading might reach its limit point to the extent of forming free radicals interfering with the reaction and reducing its efficiency (Al--shamali, 2013).

For the comparison of levels of catalyst loadings and time exposure, Figures 6 and 7 to better show the trend and their effects on the degradation of CAP during photocatalytic degradation.

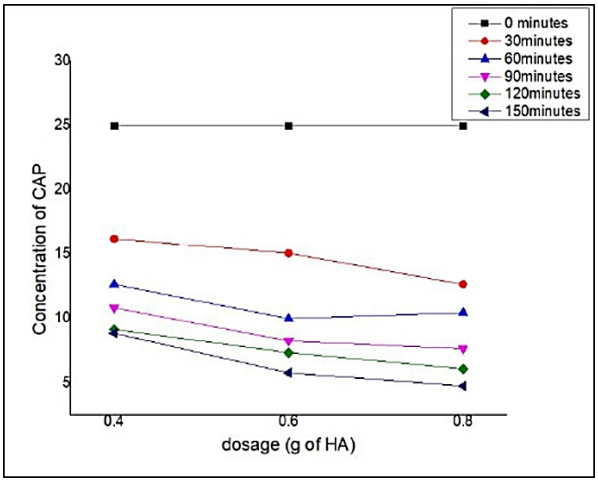

Figure 6: Comparison of the degradation for 25 mg.L^{-1} of CAP with 0.4g, 0.6g and 0.8g of catalyst dosage irradiation for 20 minutes at microwave, loadings for UV lights under different time exposure

At first two points 0.6g of HA showed close results for 0.4g dosage. It can be observed that 0.6g HA catalyst loading gave better adsorption rate than the 0.4 g HA catalyst with the increase of time. This was due to the sufficient amount of active sites as supplied by increasing the HA catalyst dosage in the degradation interaction between the CAP pollutant and the UV light (Chatzitakis., 2007). It is worth noticing that the great effect of degradation noted during the first 60 mins was 59.59% efficiency for the first 60 minutes;; and 17.82% efficiency for the next 90 minutes. This indicates that the surface of HA catalyst was slowly saturated with CAP pollutants, thus hindering the degradation rate.

With 0.8 g of catalyst the degradation went faster as compared with the other two catalyst loadings. It was observed that 0.8 g HA catalyst loading gave a higher degradation efficiencies as 80.92%. Due to the sufficient amount of catalyst that allows more active sites for the adsorption of the CAP pollutant thus ensuring a higher degrade rate (Chatzitakis., 2007). This means that 0.8 g of HA catalyst irradiated for 20 minutes can remove 81% of 25 mg.L^{-1} CAP in 250ml of spiked waste water.

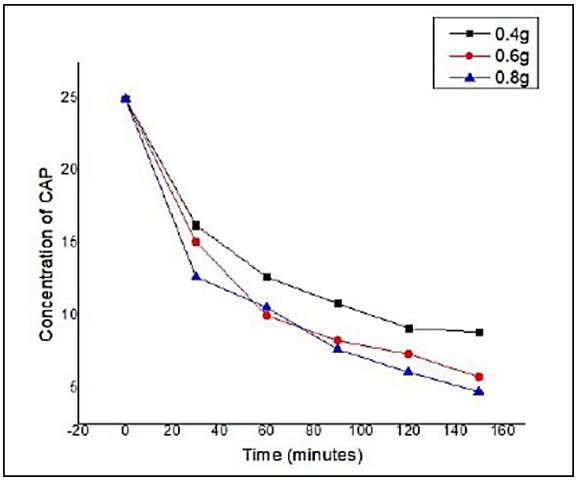

Figure 7: Comparison of the degradation for 25 mg.L^{-1} of CAP with 0.4, 0.6 and 0.8g catalyst loadings under different time exposure

Figure 7 shows all experimental runs from 0 minutes to 2.5 hours with an interval of 0.5 hours. For the first 30 minutes, the degradation rate was too high which reduced the concentration of CAP from 25 mg.L^{-1} to 13 mg.L^{-1} in average. For the next three intervals at 60, 90 and 120 minutes, the degradation dropped down with 8% efficiency and the concentration of CAP went down at 2 mg.L^{-1} per 30 minutes. At the last point at 150 minutes, the degradation was almost the same with the first two dosages of catalyst 0.4 g and 0.6 g which show a slightly change in adsorption rate count as 6%;; but the largest effect in degradation efficiency was observed in the comparison of 0.8 g catalyst loading with the irradiation at 20 minutes in microwave.

Apparently, the huge difference in degradation efficiency was obtained at the dosage of 0.8 g HA catalyst irradiated at 20 minutes reducing the concentration of CAP from 24.95 mg.L^{-1} to 4.76 mg.L^{-1}. Lastly, the addition of 0.8 g HA catalyst with irradiation time of 20 minutes can be used as a significant factor to consider in degrading CAP pollutant using photocatalysis, and the time with respect to its absorbance rate gave the most effective degradation at 2.5 hours of exposure. Moreover, the time exposure for the degradation noted a major effect in the first 60 minutes which may decrease the signification of time exposure for the last 150 minutes (Vijayabalan, Selvam, Krishnakumar, and Swaminathan, 2013).

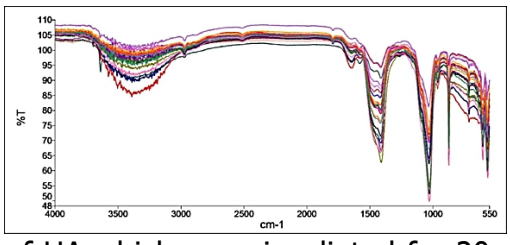

Figure 8: The FTIR result of HA which were irradiated for 20 minutes, compared to the same catalyst after the process of degradation

Figure 8 shows all of the degradation graph of the different catalyst after the degradation process using FTIR. The results show the extend of the beaks because of the degradation effect with respect to the increase of UV light exposure time up to

2.5 hours. Moreover, the extending showed clearly at the hydroxyl radicals falling at the range of 3643 cm--1 to 3330.53 cm--1;; while the other peaks falling between 640 cm--1 to 500.98 cm--1 showed a degradation extend as well (Dewidar, Nosier, and El--Shazly, 2018).

Statistical Analysis

ANOVA determined the significant factors for the 18 samples to confirm the significant effect of the variables (the catalyst loading and/or UV light time of exposure) using Two--way ANOVA analysis in finding its effectiveness on the CAP degradation while undergoing photocatalytic process.

Table 2: ANOVA Results of the Effect of Catalyst Dosage and Time Exposure Variations on Degradation of CAP

Source	Degree of Freedom	Adjusted Sum of Square	Adjusted Mean Square	F--Value	P--Value
Exposure Time	5	1912.940733	141.241	6.070781664	0.844498447
Catalyst Dosage	3	17630.6433	11.212	0.395211179	0.006471668
Exposure Time & Catalyst Dosage	15	14520.9005	0.754	--	--
Total	23	34064.48453	--	--	--

The Effect is Considerable with the p--value<0.05
The Effect is not Considerable with the p--value>0.05

Table 2, shows the amounts of p--value that are equal to 0.006 which determined that the dosage of catalyst mixed with CAP was a considerable factor causing a significant effect on the degradation process, with p--values less than 0.05 showing the reaction of all parameters were also validated to have significant effects on photocatalytic degradation of CAP. The table also presents the p--value that is equal to 0.84 which determined the exposure time under UV lights has no significant effect on the degradation process. Due to high adsorption CAP ability on HAp surfaces within the first 60 minutes. The next 90 minutes had insignificant effect, as shown in Figure 7 in accordance with the study of O'Shea, et al. and Dewidar, et al, (2018).

Kinetic Study of the Photocatalytic Degradation of CAP

The kinetic experiments with varying parameters (catalysis dosage and exposure time to UV lights) determined the observed coefficient of its reaction rate. In general, all three dosage amount showed good results for the degradation process based on the kinetic study.

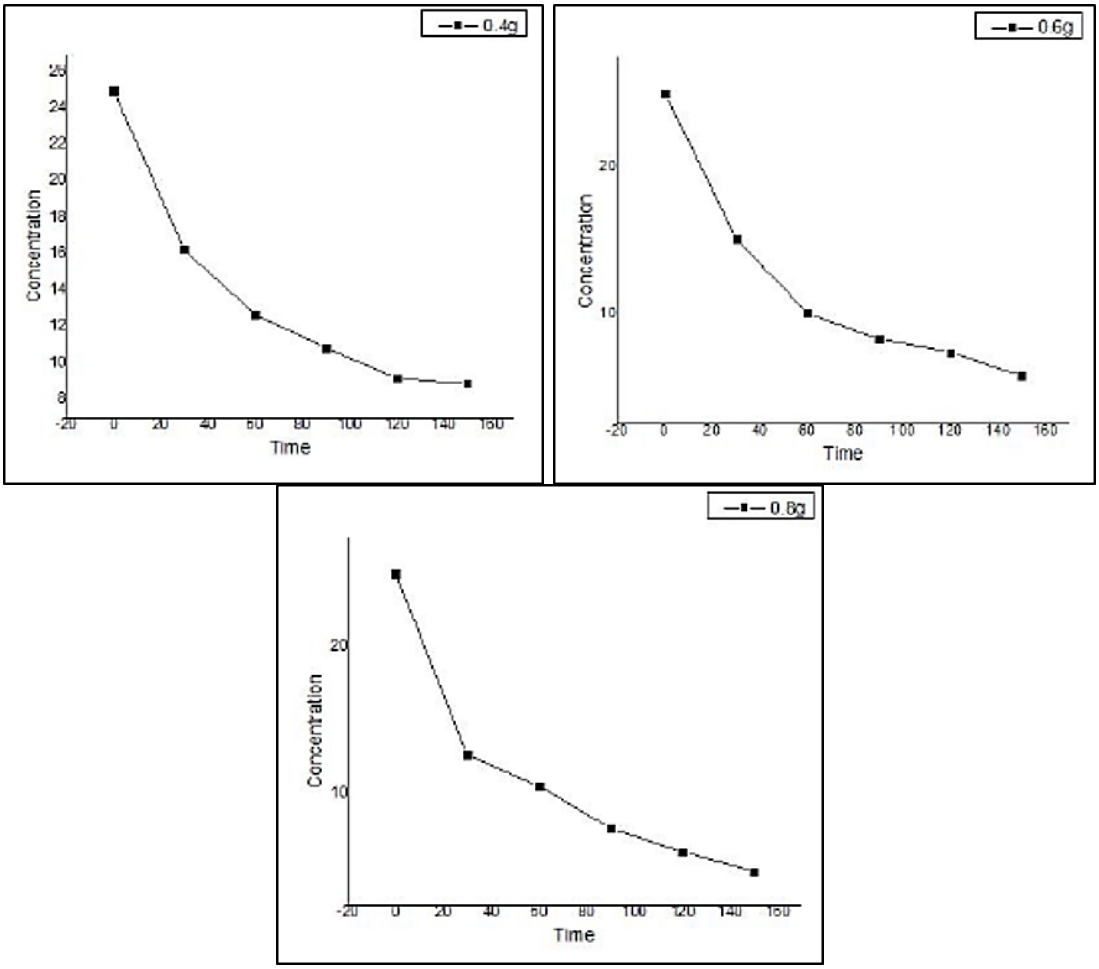

Figure 9: Zeroth Order for the Chemical Kinetics Rate for CAP Degradation using Hydroxyapatite Powder

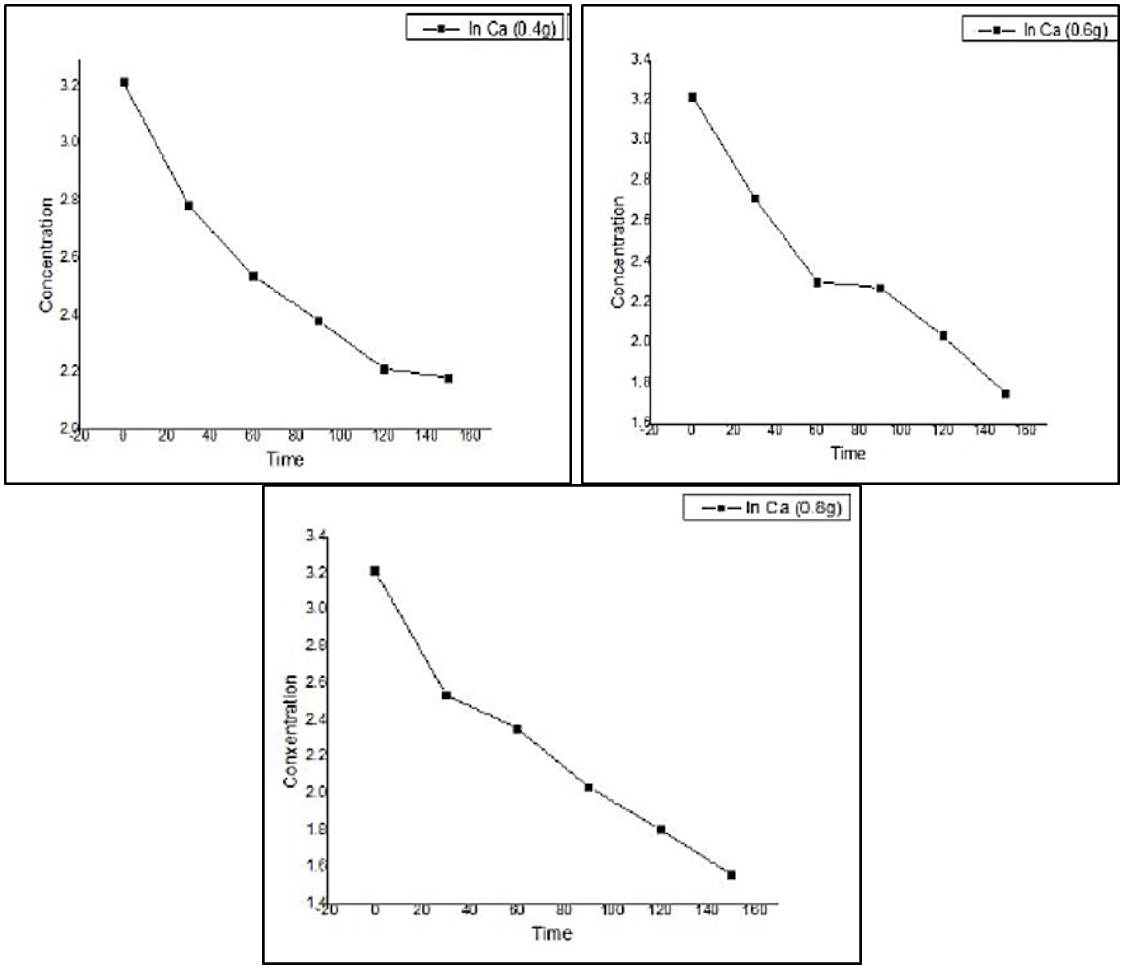

Figure 10: First Order for the Chemical Kinetics Rate for CAP Degradation using Hydroxyapatite Powder

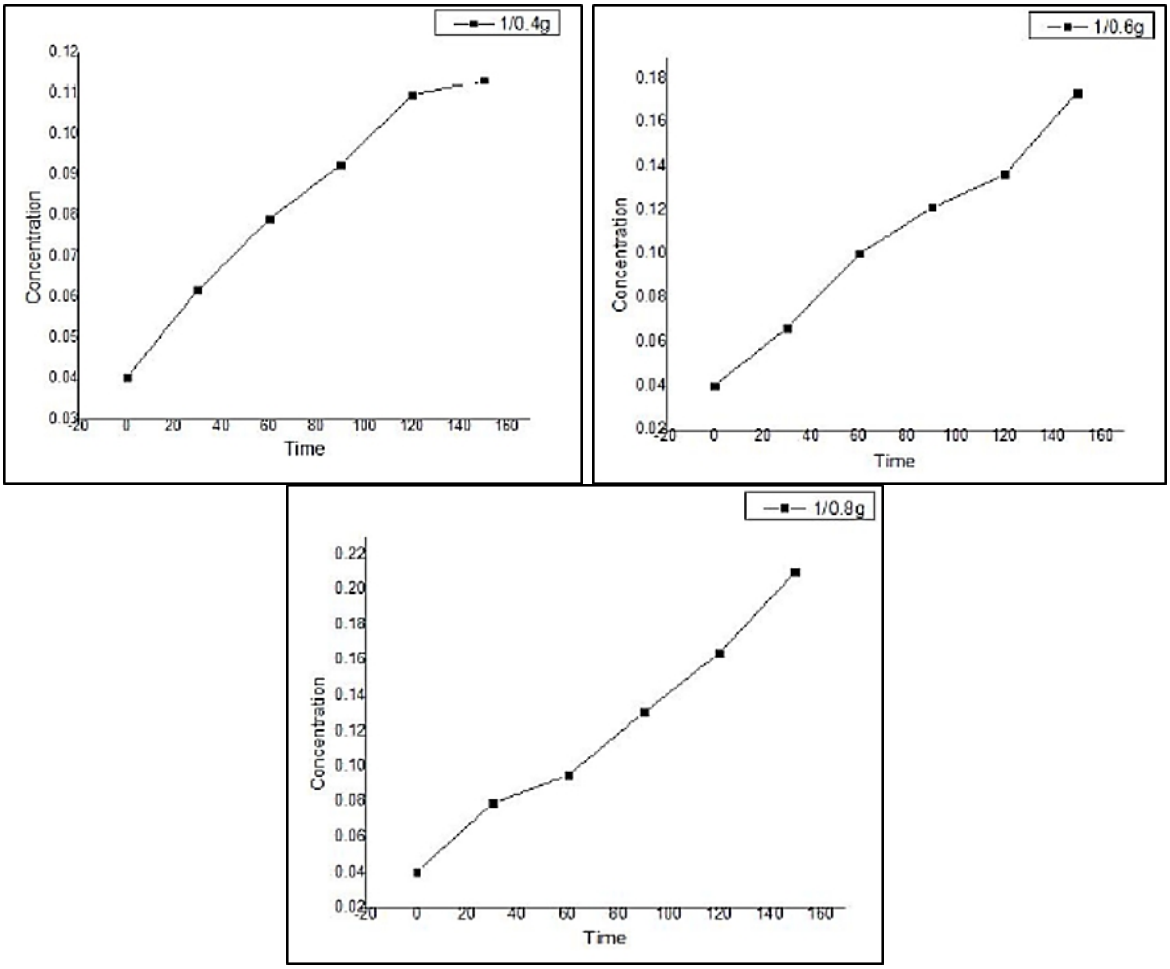

Figure 11: Second Order for the Chemical Kinetics Rate for CAP Degradation using Hydroxyapatite Powder

The linear equation was applied also to compare between the linearization of the reaction based on K factor. On Table 4.4, the rates of R^2 were compared for the zeroth and first order to see the best fit model for CAP degradation process.

Table 3: Influence of catalyst dosage and irradiation time in the degradation of CAP

Catalyst dosage	0.4 g	0.6 g	0.8 g
Zero Order	0.8210	0.8514	0.8022
First Order	0.9949	0.9664	0.9797
Second Order	0.9132	0.9363	0.9531
Model of Best Fit	1st Order	1st Order	1st Order

(Mandal et al., 2009) the photocatalytic degradation for CAP follows the first--order model. Table 3 shows a close result for first and second orders. However, this study considered the first order reaction.

The diffusion of catalyst and degradation of CAP can be applied for the first order Linear equation. The highest K factor shows the best result in the first kinetic study to describe the most efficient dosage, with exposure time under UV light. The first order kinetic equation illustrated (4.1):

$$Ln[C]_t = --k\,t + ln[C]_0 \qquad (4.1)$$

Where C_i is the concentration of chloramphenicol in mg/L, t denotes the time in the unit of seconds (s)$_{ii}$ and k denotes the coefficient for the reaction rate observed in s^{-1}, $[C]_t$ is the CAP concentration at time t and $[C]_0$ concentration at time zero.
The Eq. (4.1) was compared with other equation on Figure 4.10, for all the best degradation results of first order kinetics was confirmed. (Xia, Gu, Zhang, Zhang, and Hermanowicz, 2014).

For 0.4g of catalyst dosage

$$[y = --0.0067x + 3.0565] \qquad (4.2)$$

For 0.6g of catalyst dosage

$$[y = --0.0089x + 3.0521] \qquad (4.3)$$

For 0.8g of catalyst dosage

$$[y = --0.0103x + 3.0232] \qquad (4.4)$$

The K factor was found in equations (4.2), (4.3), and (4.4) after it fit with equation (4.1) for the catalyst dosage 0.4g;; 0.6g;; and 0.8g were 0.0067;; 0.0089;; and 0.0103 in a row. However, 0.8 g gave good kinetic degradation with higher K factor, and made it the best kinetic degradation for this study.

5.0 CONCLUSIONS AND RECOMMENDATIONS

5.1 CONCLUSIONS

In this study, it was found out that the produced hydroxyapatite from eggshells via calcination was proven to degrade CAP during photocatalytic degradation based on the following findings.

The FTIR spectra with respective peaks showed the presence functional groups of hydroxyapatite (HA), and was further confirmed by the special bands of the apatite falling in between the range of 3670 m^{-1} to 545 $m^{-1}$for all function groups of HA.

SEM analysis showed the surface morphology of HA composed of micro and nano crystalline falling within the range of 0.1 to 1 micrometer. Considering the best HA that has the irradiation time of 20 minutes, its range falls around 0.1 to 0.5 micrometers. Moreover, its structure appeared in irregular shapes agglomerated that endorse its morphology in terms of blocks.

The XRD results of the HA showed that all peaks confirmed the presence of HA based on the XRD Match Data Based. The results were confirmed based on the findings of the previous studies. Moreover, the XRD spectra established that the 20 minutes as the best irradiation time based on the least number of unmatched peaks.

The highest degradation efficiency that was achieved for CAP was 80.92% and 78.19 which was acquired at 25 $mg.L^{-1}$ with 0.8 g of HA catalyst irradiation for 20 minutes at microwave respectively for 2.5 hours of exposure under UV lights. Thus, the dosage levels obtained the higher degradation efficiencies using the HA with 20 minutes irradiation time and 150 minutes of UV exposure in the degradation of CAP.

The Two--way ANOVA determined the significant effect of the factors influencing the efficiency of the photocatalytic degradation by generating the p--values. Furthermore, the results have shown that the catalyst dosage were the factors considered to has a significant effect;; while the UV light time exposure had insignificant effect which was due to adsorption time for the pollutant on the catalyst surface to reach high percentage of the catalyst saturation less than 150 minutes.

The kinetic study, shows that the behavior of the reaction followed the first order as the best fit model. Moreover, all equations of hydroxyapatite dosage were determined by plotting the first order reaction. In this study, 0.8 g was found to be the best model for 0.8 g of HA with the k factor denoted at 0.0103.

5.2 RECOMMENDATIONS

For future research reference works, this study can completely enhance the synthesis of HA from eggshells. Factors such as calcination time may be reduced to save energy. Moreover, different parameters or media such as the Hydroxyapatite saturation and different kind of antibiotics, pollutant concentration, and weather conditions may be altered. Addition of the oxidizing agents is possibly another factor since it would affect its effectiveness in degradation which may be more active for the release of its free radicals that are reactively high.

Future researchers may use a spiked wastewater with other compounds or contaminants present. The study has its potential to be developed and/or applied if an actual wastewater would be used. The findings of this study could be applied at the pharmaceutical plants and antibiotic manufacturing industries.

Finally, a feasibility study may be conducted in terms of the results and costs. The sustainability and preservation of the environment is part of the researcher's responsibility. Therefore, wastes must either be minimized in conducts this study, or utilize other sources of waste to reduce the hazard to its surrounding.

6.0 REFERENCES

Ahmadi, M., Ramezani, H., & Jaafarzadeh, N. (2017). *Enhanced photocatalytic degradation of tetracycline and real pharmaceutical wastewater using MWCNT / TiO 2 nano--composite,* (2016), 1–9. https://doi.org/10.1016/j.jenvman.2016.09.088

Al--shamali, S. S. (2013). *Photocatalytic Degradation of Methylene Blue in the Presence of TiO 2 Catalyst Assisted Solar Radiation*, 7(4), 172–176.

Arami, H., Mohajerani, M., Mazloumi, M., Khalifehzadeh, R., Lak, A., & Sadrnezhaad, S. K. (2009). Rapid formation of hydroxyapatite nanostrips via microwave irradiation.

Journal of Alloys and Compounds, 469(1–2), 391–394. https://doi.org/10.1016/j.jallcom.2008.01.116

Autónoma, U., Química, F. De, Concordia, C. A., & Carmen, C. (2011). *Photocatalytic Degradation of Acetaminophen*, 5(4), 1071–1078.

Berzina--Cimdina, L., & Borodajenko, N. (2012). *Research of Calcium Phosphates Using Fourier Transform Infrared Spectroscopy.* Infrared Spectroscopy -- Materials Science, Engineering and Technology. https://doi.org/10.5772/36942

Bhatkhande, D. S., Pangarkar, V. G., & Beenackers, A. A. C. M. (2002*). Photocatalytic degradation for environmental applications* – a review, 116(March 2001). https://doi.org/10.1002/jctb.532

Bramhe, S., Nam, T., Balakrishnan, A., & Cheol, M. (2014). Conversion from biowaste Venerupis clam shells to hydroxyapatite nanowires. *Materials Letters*, 135, 195–198. https://doi.org/10.1016/j.matlet.2014.07.137

Cengiz, B., Gokce, Y., Yildiz, N., Aktas, Z., & Calimli, A. (2008). *Colloids and Surfaces A : Physicochemical and Engineering Aspects Synthesis and characterization of hydroxyapatite nanoparticles,* 322, 29–33. https://doi.org/10.1016/j.colsurfa.2008.02.011

Chatzitakis, A., Berberidou, C., Paspaltsis, I., Kyriakou, G., Sklaviadis, T., & Poulios, I. (2008). Photocatalytic degradation and drug activity reduction of Chloramphenicol. *Water Research*, 42(1–2), 386–394. https://doi.org/10.1016/j.watres.2007.07.030
Cox, A. S. (n.d.). Synthesis Method of Hydroxyapatite.

D. C. O'Shea. M. L. Bartlett and R. A. Young (1974), *Compositional Analysis Of Apatites With Laser..Raman Spectroscopy (Oh,F,Cl)Apatites*

Dewidar, H., Nosier, S. A., & El--Shazly, A. H. (2018). Photocatalytic degradation of phenol solution using Zinc Oxide/UV. *Journal of Chemical Health and Safety*, 25(1), 2–11. https://doi.org/10.1016/j.jchas.2017.06.001

Dfs, F. D. A. O. R. A., Neuhaus, B. K., Hurlbut, J. A., & Hammack, W. (n.d.). LC / MS / MS Analysis of Chloramphenicol in Shrimp, (4290).

Dong, H., Zeng, G., Tang, L., Fan, C., Zhang, C., He, X., & He, Y. (2015). An overview on limitations of TiO<inf>2</inf>--based particles for photocatalytic degradation of organic pollutants and the corresponding countermeasures. *Water Research*, 79, 128–146. https://doi.org/10.1016/j.watres.2015.04.038

Doorslaer, X. V. A. N., Demeestere, K., Heynderickx, P. M., & Caussyn, M. (2013). *Photocatalytic Degradation Of The Antibiotic Moxifloxacin : A Deeper Look At The Degradation Products And Residual Antibacterial Activity*, (September), 5–7.

Dunlop, P. S. M., Ciavola, M., Rizzo, L., Mcdowell, D. A., & Byrne, J. A. (2014*). Effect of photocatalysis on the transfer of antibiotic resistance genes in urban wastewater. Catalysis Today*, 10–15. https://doi.org/10.1016/j.cattod.2014.03.049

Elmolla, E. S., & Chaudhuri, M. (2010). *Photocatalytic degradation of amoxicillin , ampicillin and cloxacillin antibiotics in aqueous solution using UV / TiO 2 and UV / H 2 O 2 / TiO 2 photocatalysis. DES*, 252(1–3), 46–52. https://doi.org/10.1016/j.desal.2009.11.003

Espino, M. P. B. (2008). *Photolytical Degradation Products of Pentachlorophenol in Aqueous Solution and Organic Solvents*, 137(December), 179–188.

Gap, B. (n.d.). What is Photocatalyst ? Photocatalytic Oxidation Photocatalytic Oxidation, 1240.

Gilmour, C. (2012). *Water Treatment using Advanced Oxidation Processes : Application Perspectives,* (September), 1–111.

Giraldo--aguirre, A. L., Erazo--erazo, E. D., Flórez--acosta, O. A., Serna--galvis, E. A., & Torres--palma, R. A. (2015). Journal of Photochemistry and Photobiology A : Chemistry TiO 2 photocatalysis applied to the degradation and antimicrobial activity removal of oxacillin : Evaluation of matrix components , experimental parameters , degradation pathways and identificatio. *"Journal of Photochemistry & Photobiology, A: Chemistry,"*311, 95–103. https://doi.org/10.1016/j.jphotochem.2015.06.021--

Hassena, H. (2016). *Photocatalytic Degradation of Methylene Blue by Using Al2O3/Fe2O3 Nano Composite under Visible Light. Modern Chemistry & Applications*, 4(1), 3–7. https://doi.org/10.4172/2329--6798.1000176

Hatim, N. A., & Ahmad, Z. M. (2013*). A Novel Method for Conversion of Eggshell Hydroxyapatite Particles to Nano--size Using Microwave Irradiation*, 2(11), 71–76.

Ibrahim, A. R., Wei, W., Zhang, D., Wang, H., & Li, J. (2013). Conversion of waste eggshells to mesoporous hydroxyapatite nanoparticles with high surface area. *Materials Letters*, 110, 195–197. https://doi.org/10.1016/j.matlet.2013.08.014

Iqbal, H., Ali, M., Zeeshan, R., Mutahir, Z., Iqbal, F., Nawaz, M. A. H., … Rehman, I. ur. (2017). *Chitosan/hydroxyapatite (HA)/hydroxypropylmethyl cellulose (HPMC) spongy scaffolds--synthesis and evaluation as potential alveolar bone substitutes. Colloids and Surfaces B: Biointerfaces*, 160, 553–563. https://doi.org/10.1016/j.colsurfb.2017.09.059

Islam, M., Chandra, P., & Patel, R. (2010). Physicochemical characterization of hydroxyapatite and its application towards removal of nitrate from water*. Journal of Environmental Management,* 91(9), 1883–1891. https://doi.org/10.1016/j.jenvman.2010.04.013

Jay, E., Edralin, M., Garcia, J. L., Francis, M., & Punzalan, E. R. (2017). Sonochemical synthesis , characterization and photocatalytic properties of hydroxyapatite nano--rods derived from mussel shells. *Materials Letters*, 10, 1–8. https://doi.org/10.1016/j.matlet.2017.03.016

Jun, A., Shariffuddin, H., Ian, M., Darrell, J., & Patterson, A. (2013). *Ac ce pt ed us cr t. Chemical Engineering Research and Design.* https://doi.org/10.1016/j.cherd.2013.04.018

Kumar, G. S., & Girija, E. K. (2013). *Flower--like hydroxyapatite nanostructure obtained from eggshell: A candidate for biomedical applications.* Ceramics International, 39(7), 8293–8299. https://doi.org/10.1016/j.ceramint.2013.03.099

Kumar, G. S., Thamizhavel, A., & Girija, E. K. (2012). *Microwave conversion of eggshells into fl ower--like hydroxyapatite nanostructure for biomedical applications.* Materials Letters, 76, 198–200. https://doi.org/10.1016/j.matlet.2012.02.106

Lee, S., Kim, S., Balázsi, C., & Chae, W. (2012). *Comparative study of hydroxyapatite from eggshells and synthetic hydroxyapatite for bone regeneration*. OOOO, 113(3), 348–355. https://doi.org/10.1016/j.tripleo.2011.03.033

Lin, Z., Hu, R., Zhou, J., Ye, Y., Xu, Z., & Lin, C. (2017). A further insight into the adsorption mechanism of protein on hydroxyapatite by FTIR--ATR spectrometry. *Spectrochimica Acta -- Part A: Molecular and Biomolecular Spectroscopy,* 173, 527–531. https://doi.org/10.1016/j.saa.2016.09.050

Liu, J., Li, K., Wang, H., Zhu, M., & Yan, H. (2004). Rapid formation of hydroxyapatite nanostructures by microwave irradiation. *Chemical Physics Letters*, 396(4–6), 429–432. https://doi.org/10.1016/j.cplett.2004.08.094